Lawrence Berkeley National Laboratory

LBL Publications

Title

Effect of band anticrossing on the optical transitions in GaAs1-xNx/GaAs multiple quantum wells

Permalink

https://escholarship.org/uc/item/9w1759vn

Journal

Physical Review B, 64(8)

Author

Tu, C.W.

Publication Date

2000-09-01

eScholarship.org Powered by the California Digital Library
University of California

Effect of Band Anticrossing on the Optical Transitions in $GaAs_{1-x}N_x$/GaAs Multiple Quantum Wells

J. Wu,[1,2] W. Shan,[2] W. Walukiewicz,[2] K. M. Yu,[2] J. W. Ager III,[2] E. E. Haller[2,3]
H. P. Xin,[4] and C.W. Tu[4]

1. Applied Science and Technology Graduate Group, University of California, Berkeley, CA 94720

2. Materials Sciences Division, Lawrence Berkeley National Laboratory, Berkeley, CA 94720

3. Department of Materials Sciences and Engineering, University of California, Berkeley, CA 94720

4. Department of Electrical and Computer Engineering, University of California, San Diego, La Jolla, CA 92093

Interband transitions in $GaAs_{1-x}N_x$/GaAs multiple quantum wells were studied at room temperature by photo-modulated reflectance spectroscopy as a function of well width (3 - 9 nm), the nitrogen concentration ($0.012 < x < 0.028$), and hydrostatic pressure (0 - 64 kbar). All experimental data can be quantitatively explained using the dispersion relationship obtained from a band anticrossing model to calculate electron confinement effects in a finite depth quantum well. The results are consistent with a nitrogen-induced large increase of the electron effective mass in the GaAsN quantum wells.

PACS numbers: 71.20.Nr; 71.55.Eq; 78.66.Fd; 62.50.+p

Electronic mail: jqwu@socrates.berkeley.edu

Incorporation of small amounts (< 5%) of nitrogen into GaAs to form $GaAs_{1-x}N_x$ strongly reduces the fundamental band gap, resulting in a material system with band gap energies covering 1.0 - 1.42 eV [1-3]. The lattice parameter of cubic GaN is much smaller than that of GaAs and pseudomorphic $GaAs_{1-x}N_x$ layers grown on GaAs substrates are under biaxial tensile strain. Alloying of $GaAs_{1-x}N_x$ with InAs can be used to compensate the N-induced reduction of the lattice parameter. $In_yGa_{1-y}As_{1-x}N_x$ with $y=3x$ is lattice-matched to GaAs and has a similar N-induced energy gap reduction effect as that found in $GaAs_{1-x}N_x$ [3]. It has been demonstrated that practically all of the N-induced band gap reduction is accommodated by a downward shift of the conduction band edge [4]. Therefore, when $GaAs_{1-x}N_x$/GaAs or $In_yGa_{1-y}As_{1-x}N_x$/GaAs quantum wells are formed, most of the confinement energy is restricted to the electrons in the conduction band of the alloy layers. In $GaAs_{1-x}N_x$/GaAs quantum wells, a small contribution to the valence band confinement is expected from the symmetry breaking biaxial strain. The ability to control the band gaps of $In_yGa_{1-y}As_{1-x}N_x$ alloys with only very small amounts of N generates a significant interest in applications of these materials for multi-junction solar cells and long wavelength light emitters [5].

It has been shown that the incorporation of N results in a new optical absorption edge whose position strongly depends on hydrostatic pressure [6] and the N content [7]. Significant progress in understanding the effect of N on the electronic structure of III-V-N alloys has been made recently by studying the pressure dependence of the interband optical transitions in InGaAsN alloys [6]. The results of these experiments were explained by a band anticrossing (BAC) model in which a highly localized N level interacts with the extended states of the host semiconductor [6,8]. The BAC model did

not only explain the existing data but also predicted new effects that were later experimentally confirmed [9-11].

Another model for the electronic structure of GaAsN alloys has been proposed very recently [12] in the context of measuring confinement effects in GaAsN/GaAs quantum wells. This "N-impurity band" model argues that in III-V-N materials, the downward shift of the lowest conduction band is a result of the formation of an impurity band below the conduction band edge, analogous to effects observed in semiconductors doped with electrically active dopants. One conclusion of the model was the prediction of a large electron effective mass (up to 0.55 m_0 at x = 0.009) that decreases with increasing N content. This conclusion appeared to be inconsistent with some experimental observations of the effective mass in bulk GaAsN structures [11,13]. The potential for important practical applications clearly necessitates a resolution of these conflicting interpretations and a better understanding of the electronic structure of the III-V-N based quantum wells. In this paper, we report the result of our studies of interband transitions in $GaAs_{1-x}N_x$/GaAs quantum superlattices. We show that the hydrostatic pressure dependence of the optical transition energies provides a critical test for the two different models of the $GaAs_{1-x}N_x$ electronic structure.

A series of $GaAs_{1-x}N_x$/GaAs multiple QWs with different $GaAs_{1-x}N_x$ well thickness from 3 to 9 nm, N concentrations $0.012 < x < 0.028$, and 20 nm GaAs barriers were grown by gas-source molecular beam epitaxy on semi-insulating GaAs substrate and capped by a 50 nm GaAs layer [14]. Photo-modulated reflectance spectroscopy (PR) was performed at room temperature. A chopped HeCd laser beam (325 nm or 442 nm) provided the modulation, and a halogen tungsten lamp dispersed by a 0.5 m

monochromator was used as the probe beam. The hydrostatic pressure was generated using a gasketed diamond anvil cell and calibrated by a small chip of ruby placed in the pressurized volume.

The PR spectra for GaAsN/GaAs QWs with 7nm well width and four different N concentrations are shown in Fig. 1 (a). The feature at 1.42 eV arises from the GaAs cap layer and barriers. Two transitions at lower energies are also clearly observed. We assign them to transitions from the GaAsN valence band to the two confined subbands of the conduction band and denote them E_1 and E_2. As shown in Fig. 1 (b), both transitions shift to lower energy with increasing x, corresponding to the bandgap reduction observed in bulk $GaAs_{1-x}N_x$ [1-3, 7]. We also note that the data in Fig. 1 and in Fig. 2 below agree, to within experimental error, to similar data presented in Ref. [12].

In first order perturbation theory, the BAC model predicts a hybridized lowest conduction band given by [6,8]

$$E_{-}(k)=\frac{1}{2}\left[\left(E_M(k)+E_N\right)-\sqrt{\left(E_M(k)-E_N\right)^2+4C_{NM}{}^2x}\right], \qquad (1)$$

where C_{NM}=2.7eV describes the interaction strength between the N level E_N and the conduction band of GaAs, $E_M(k)$. The N level has been determined to lie at ~0.23 eV above the GaAs conduction band edge at room temperature [6], and the GaAs conduction band near the Γ point can be well represented by a parabolic dispersion function with effective electron mass m^*_{GaAs}=0.067 m_0. The band gap of bulk $GaAs_{1-x}N_x$ given by Eq. (1) agrees well with experiments [6] and is plotted in Fig. 1 (b). It can be seen that the ground-level transition in the QW, E_1, is blue shifted from the bulk energy gap due to quantum confinement.

To evaluate the confinement quantitatively, we applied a finite-depth single square well confinement model with the depth and width of the well and the effective mass inside and outside the well as input parameters. The electron dispersion given by Eq. (1) is non-parabolic, such that the electron effective mass in the conduction band is dependent on the *k* vector, which results in an inseparable Schrödinger equation. To simplify the calculation, we have assumed that the effective mass of the electrons in the quantum well can be approximated by an energy-independent density-of-states mass at the bottom of the lowest conduction band [8,11],

$$m^* \approx \hbar^2 \left| \frac{k}{dE_-(k)/dk} \right|_{k=0} = 2\, m^*_{GaAs} \Bigg/ \left[1 - \frac{E_M(0) - E_N}{\sqrt{(E_M(0) - E_N)^2 + 4\, C_{NM}{}^2 x}} \right]. \qquad (2)$$

This approximation can be justified by the fact that the confined states are close to the bottom of the conduction band (see Fig. 1 (b)). Changes of the effective mass of less than 5% and 15% are estimated for the ground state and first excited state energies , respectively.

Photoluminescence [15] and x-ray photoelectron spectroscopy [16] studies of $GaAs_{1-x}N_x$/GaAs heterostructures indicate a slightly type-II band lineup with a very small negative valence-band offset of $|\Delta E_v| < 20$meV/%N. For this type-II band lineup, the transition energies are not sensitive to the value of the valence band offset, because the holes are not confined in the active well layer. Consequently, the lower states of the optical transitions in the well are always located at the top of the valence band, and the energies of the two observed transitions are given by the locations of the ground and first excited states of the confined conduction band electrons [15]. For $x<0.03$, the lattice constant of $GaAs_{1-x}N_x$ changes from that of GaAs by less than 0.5% [17]. The biaxial

tensile strain introduced by this small mismatch may raise the valence bands of $GaAs_{1-x}N_x$ by 40 meV at most [18]. The quantum confinement on the holes by this shallow well has been estimated to decrease the transition energies by less than 20 meV for all the QWs studied in this paper. It is important to note that the small energy shifts resulting from the biaxial strain-induced hole confinement do not depend on the external hydrostatic pressure and are the same for all the optical transitions observed. Also, the maximum energy shift is equivalent to the shift produced by a change of the N content of less than 0.2 %, which is below the accuracy of the determination of the alloy composition. We can therefore argue that the conclusions of this paper are not affected by the omission from our model of the effect of strain on the valence band offsets.

The calculated energies of E_1 and E_2 found using the well depth and QW effective mass obtained from Eqs. (1) and (2) are shown as solid curves in Fig. 1 (b). The calculations are in good agreement with the experimental results. The agreement is even more remarkable considering the fact that no adjustable parameters have been used in the calculations. That is, we have used parameters (e.g. E_N and C_{MN}) that were previously determined from the studies of the composition and pressure dependence of the optical properties of InGaAsN alloys [6,8]. For all the four samples shown in Fig.1, the effective mass calculated from Eq. (2) is equal to about $0.11m_0$, which is over 60% larger than the electron effective mass of GaAs. To demonstrate the effect of the heavier electron mass, we have also calculated the optical transition energies assuming that the electron effective mass of GaAsN alloys is the same as that of GaAs. The results are shown as dashed curves in Fig. 1 (b). Clearly, much better agreement with the experiment is reached when the N-induced enhancement of the electron effective mass is incorporated in the model.

Similar values of the effective mass have been theoretically predicted [19] and experimentally observed before. Jones and coworkers measured via three different techniques an effective mass of ~$0.13m_0$ for $In_{0.07}Ga_{0.93}As_{0.98}N_{0.02}$ [13]. Hetterich *et. al.* observed an effective mass increased by ~$0.03m_0$ in a InGaAsN alloy with 1.5% N [20]. All these independent results agree reasonably well with the values predicted by Eq. (2), but are in disagreement with the much larger values (from $0.55m_0$ at x=0.009 to $0.40m_0$ at x=0.020) deduced from the N-impurity band model [12].

Figure 2 shows the optical transition energies as a function of the well width for a fixed N concentration, x=0.016. The data clearly show increasing quantum confinement with decreasing well width. Again, the theoretical calculations agree well with the measured data if the heavier effective mass given by Eq. (2) is used in the calculations as opposed to a fixed value of $0.067m_0$. The effect of the heavier effective mass is especially pronounced for the optical transitions to the first excited state in the well (E_2).

The hydrostatic pressure dependence of the E_1 transition is shown in Fig. 3 along with the predicted pressure dependence of the GaAsN conduction band edge E_{bulk}. Similar to the case at ambient pressure, the pressure-dependence of E_{bulk} can be calculated with Eq. (1) by using the known pressure dependencies of E_M and E_N. It can be seen that the confinement energy, E_1-E_{bulk}, decreases with increasing pressure. This effect is a result of the pressure-induced increase of the electron effective mass predicted by the BAC model [8]. Because of the much different pressure coefficients of the extended states (dE_M/dP=10.8meV/kbar) and the localized N states (dE_N/dP=1.5meV/kbar)[6,8], the conduction band edge shifts towards E_N under hydrostatic pressures. According to Eqs. (1) and (2), this shift leads to a flattening of the dispersion relation and an increase

of the electron effective mass in the lowest conduction band. For the sample in Fig. 3, the effective mass increases from $0.11m_0$ at ambient pressure to $0.28m_0$ at 70 kbar, four times larger than the effective mass of the GaAs host. It is also evident from Fig. 3 that, as shown by the dashed curve, the calculations assuming a pressure-independent effective mass are in disagreement with the experimental results at high pressures. The increase of electron effective mass with pressure has also been reported in Ref [13].

The pressure dependence of the E_1 level provides a critical test for the different theoretical models of the electronic band structure of III-V-N alloys. According to the N-impurity band model, the conduction band edge is formed by the states of N atom *clusters* [12]. Previous measurements have shown that the pressure dependence of the energy levels of the N-clusters is very weak and is ~5meV/kbar at ambient pressure and *continuously decreases* with pressure to ~3.5 meV/kbar at P~30 kbar [21]. Within the N-impurity band model, since the spatial overlaps between the highly localized wave functions of different clusters do not depend strongly on pressure, it is expected that the conduction band edge should also have a similarly small pressure coefficient, and the effective mass should not depend on pressure. As shown in Fig. 3, the pressure dependence predicted by the N-impurity model is much weaker than the experimental data [21].

In summary, the optical transitions from the valence band to the ground and first excited subband in $GaAs_{1-x}N_x$/GaAs multiple quantum wells have been studied by photo-modulation spectroscopy. The dependencies of the transition energies on the well width, the N concentration, and hydrostatic pressure have been investigated and discussed. The results show an increase of the electron effective mass to $\sim 0.11m_0$ for $0.012<x<0.028$ in

the $GaAs_{1-x}N_x$ layer due to the anticrossing of the N localized states and the conduction band of the host. This effective mass also increases with hydrostatic pressure.

One of the authors (J.W.) acknowledges the Berkeley Fellowship from the University of California, Berkeley. The work at LBNL is part of a project on the "Photovoltaic Materials Focus Area" in the DOE Center of Excellence for the Synthesis and Processing of Advanced Materials, Office of Science, Office of Basic Energy Sciences, Division of Materials Sciences under US Department of Energy Contract No. DE-AC03-76SF00098. The work at UCSD was partially supported by Midwest Research Institute under subcontractor No. AAD-9-18668-7 from NREL.

REFERENCES

[1] M. Weyers, M. Sato and H. Ando, Jpn. J. Appl. Phys., **31**, L853 (1992).

[2] W.G. Bi and C.W. Tu, Appl. Phys. Lett., **70**, 1608 (1997).

[3] M. Kondow, T. Kitatani, M.C. Larson, K. Narahara, K. Uomi and H. Inoue, J. Cryst. Growth, **188**, 255 (1998).

[4] W. Shan, W. Walukiewicz, W. W. Ager III, E. E. Haller, J. F. Geisz, D. J. Friedman, J. M. Olson, and Sarah R. Kurtz, J. Appl. Phys., **86**, 2349 (1999); P. J. Klar, H. Grüning, W. Heimbrodt, J. Koch, F. Höhnsdorf, W. Stolz, P. M. A. Vicente and J. Camassel, Appl. Phys. Lett., **76**, 3439, (2000).

[5] M. Kondow, K. Uomi, A. Niwa, T. Kitatani, S. Watahiki, and Y. Yazawa, Jpn. J. Appl. Phys. **35**, 1273 (1996); T. Miyamoto, K. Takeuchi, F. Koyama, and K. Iga, IEEE Photonics Tech. Lett., **9**, 1448 (1997).

[6] W. Shan, W. Walukiewicz, J.W. Ager III, E.E. Haller, J.F. Geisz, D.J. Friedman, J.M. Olson, and S.R. Kurtz, Phys. Rev. Lett., **82**, 1221 (1999).

[7] J.D. Perkins, A. Mascarenhas, Yong Zhang, J.F. Geiz, D.J. Friedman, J.M. Olson and Sarah R. Kurtz, Phys. Rev. Lett., **82**, 3312 (1999).

[8] W. Walukiewicz, W. Shan, J.W. Ager III, D.R. Chamberlin, E.E. Haller, J.F. Geisz. D.J. Friedman, J.M. Olson, and S.R. Kurtz, Proc. 195th Electrochem. Soc. Meeting, Seattle, WA, **99-11**, 190 (1999).

[9] K.M. Yu, W. Walukiewicz, W. Shan, J.W. Ager III, J. Wu, E. E. Haller, J.F. Geisz, D.J. Friedman, and J.M. Olson, Phys. Rev. B **61**, R13337 (2000)

[10] P. Perlin, P. Wisniewski, C. Skierbiszewski, T. Suski, E. Kaminska, S.G. Subramanya, E.R. Weber, D.E. Mars and W. Walukiewicz, Appl. Phys. Lett., **76**, 1279, (2000).

[11] C. Skierbiszewski, P. Perlin, P. Wisniewski, W. Knap, T. Suski, W. Walukiewicz, W. Shan, K.M. Yu, J.W. Ager III, E.E. Haller, J.F. Geisz and J.M. Olson, Appl. Phys. Lett., **76**, 2409 (2000).

[12] Yong Zhang, A. Mascarenhas, H.P. Xin, and C.W. Tu, Phys. Rev. B **61**, 7479 (2000).

[13] E.D. Jones, N. A. Modine, A. A. Allerman, I.J. Fritz, S.R. Kurtz, A.F. Wright, S.T. Tozer, and Xing Wei, Proc. 195th Electrochem. Soc. Meeting, Seattle, WA, **99-11**, 170 (1999).

[14] H.P. Xin and C.W. Tu, Appl. Phys. Lett., **72**, 2442 (1998).

[15] B.Q. Sun, D.S. Jiang, X.D. Luo, Z.Y. Xu, Z. Pan, L.H., Li and R.H. Wu, Appl. Phys. Lett., **76**, 2862, (2000).

[16] Takeshi Kitatani, Masahiko Kondow, Takeshi Kikawa, Yoshiaki Yazawa, Makoto Okai and Kazuhisa Uomi, Jpn. J. Appl. Phys., **38**, 5003 (1999); S. Tanaka, M. Takahashi, A. Moto, T. Tanabe, S. Takagishi, K. Karatani, T. Nakanishi and M. Nakayama, 25th International Symposium on Compound Semiconductors, Nara, Japan, 1998.

[17]. J. F. Geisz, D. J. Friedman, J. M. Olson, S. R. Kurtz and B. M. Keyes, J. Crystal Growth, **195**, 401, (1998).

[18] G. Ji, D. Huang, U. K. Reddy, T. S. Henderson, R. Houdre, and H. Morkoc, J. Appl. Phys. **62**, 3366 (1987).

[19] A. Lindsay and E.P. O'Reilly, Solid State Commun., **112**, 443 (1999).

[20] M. Hetterich, M.D. Dawson, A. Yu. Egorov, D. Bernklau and H. Riechert, Appl. Phys. Lett., **76**, 1030 (2000).

[21] X. Liu, E. E. Pistol, L. Samuelson, S. Schwetlick and W. Seifert, Appl. Phys. Lett., 56, 1451 (1990); J. Shen, S.Y. Ren, and J.D. Dow, Phys. Rev. B **42**, 9119 (1990).

FIGURE CAPTIONS

Fig. 1. (a) PR spectra taken at room temperature for $GaAs_{1-x}N_x$/GaAs QWs with 7 nm well width and different N concentrations. (b) First and second transition energies E_1 and E_2 as a function of N concentration for $GaAs_{1-x}N_x$/GaAs QWs with 7 nm well width. Solid curves: calculated values using band anticrossing (BAC) model and finite-depth single well confinement with $GaAs_{1-x}N_x$ electron effective mass given by Eq. (2); Short dashed curves: calculated values assuming $GaAs_{1-x}N_x$ electron effective mass equal to m^*_{GaAs}. Long dashed curve: band gap of bulk GaAsN given by BAC model, Eq. 1.

Fig. 2. E_1 (circles) and E_2 (squares) transition energies as a function of well width for x=0.016. Solid curve, calculated values with $GaAs_{1-x}N_x$ electron effective mass given by Eq. (2); Short dashed curve, calculated values assuming $GaAs_{1-x}N_x$ electron effective mass equal to m^*_{GaAs}. Long dashed lines indicates energy of bulk $GaAs_{1-x}N_x$ for x = 0.016.

Fig. 3. The first transition energy E_1 as a function of hydrostatic pressure for x=0.016 and well width=7nm. Solid curve, calculated values with $GaAs_{1-x}N_x$ electron effective mass given by Eq. (2); Short dashed curve, calculated values assuming $GaAs_{1-x}N_x$ electron effective mass equal to m^*_{GaAs}. The pressure dependencies of band edge in bulk $GaAs_{1-x}N_x$ expected from the BAC model (dot-dashed) and the N-cluster level (long dashed) from Ref. [21] are also shown.

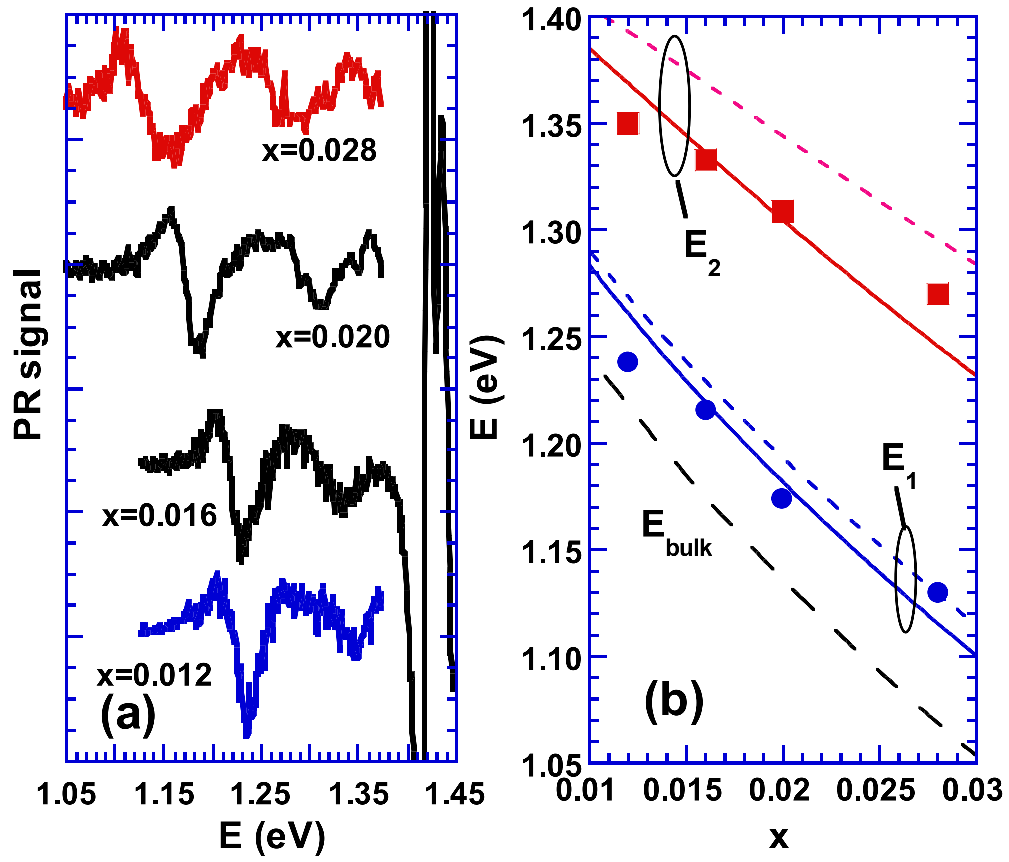

Fig. 1

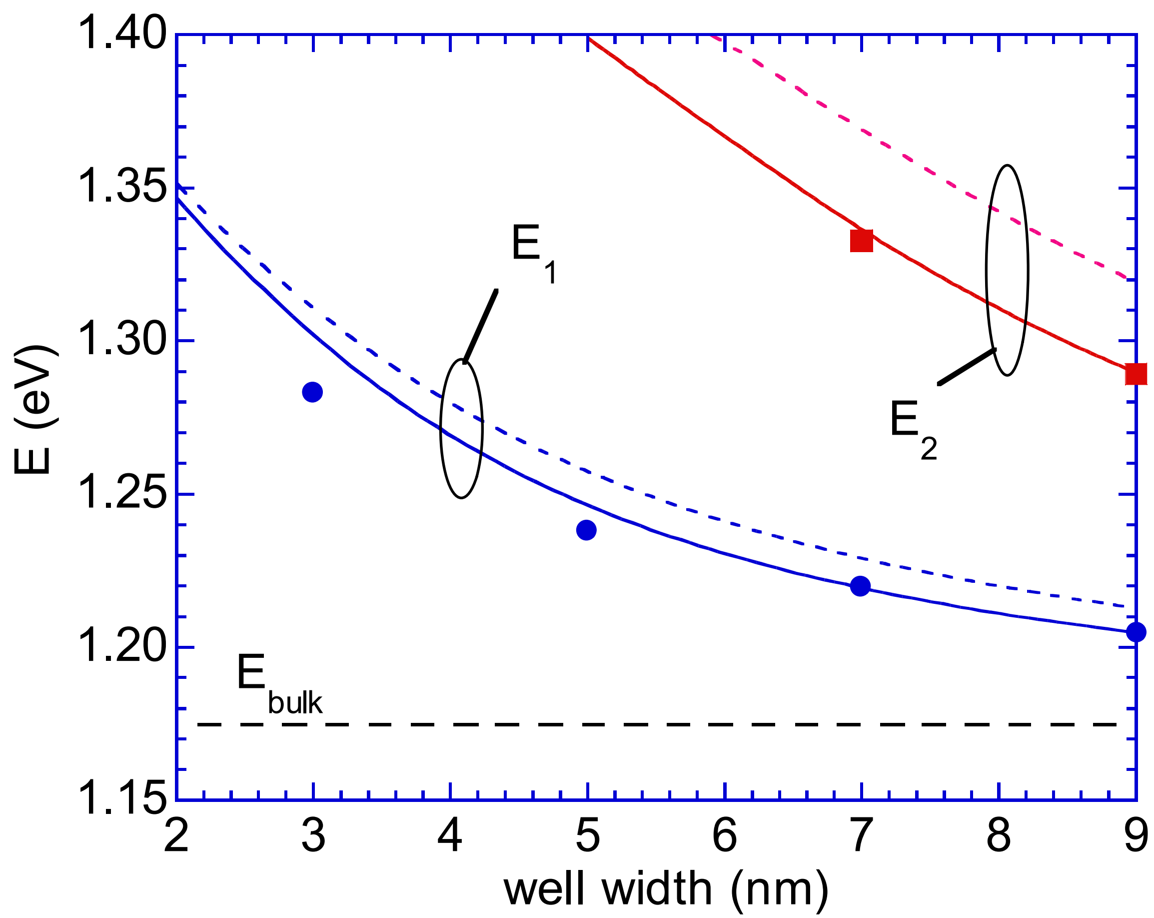

Fig. 2

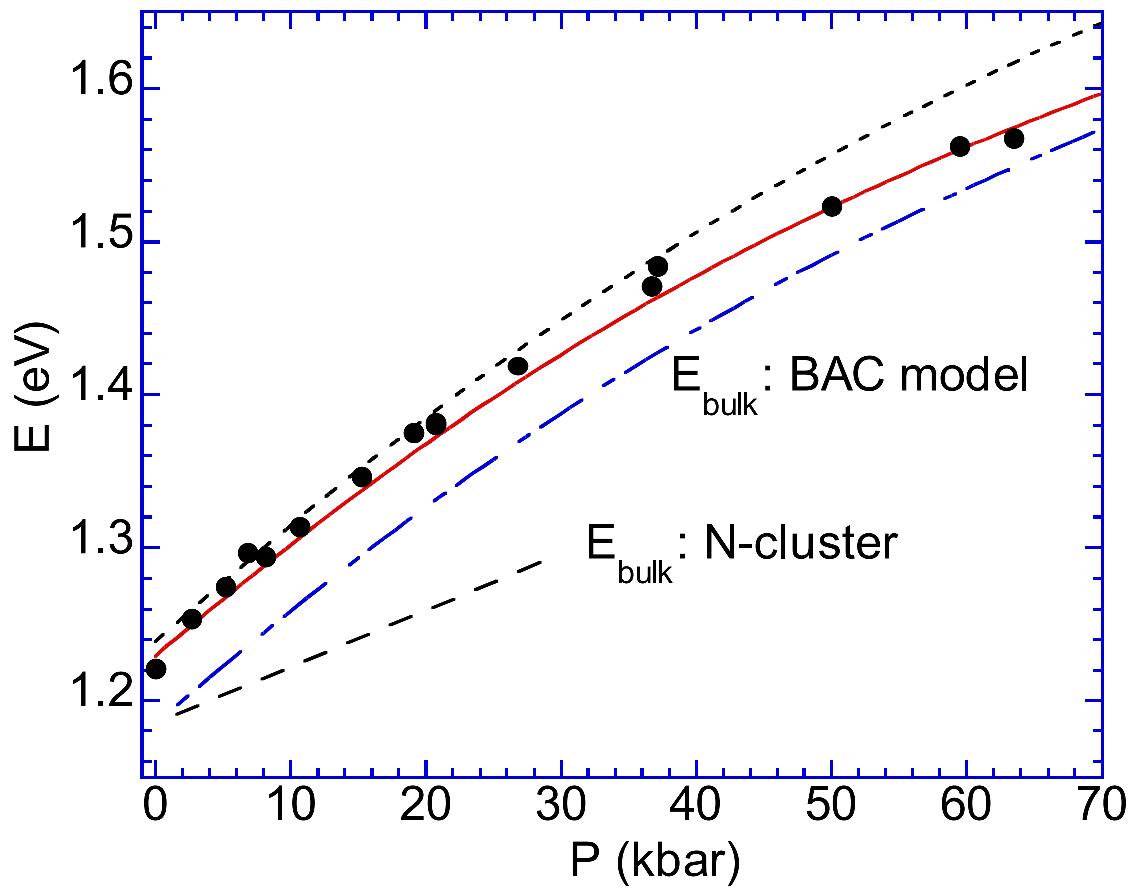

Fig. 3